

Modeling Pharmacokinetics Using Body-on-Chip Systems

Victor Cantu | Carlos Munoz | Omar Ortiz

December 17, 2017

BENG 221

1 Introduction

Pharmacokinetic studies for new therapies are often first performed in animal models or with isolated human cell lines that are cultured *in vitro* [1]. However, with 85% of treatments failing in early clinical stages and only 50% of therapies failing to make it through Phase III trials [2], it is clear that new methodologies that will better predict a drugs safety and efficacy are needed. Additionally, animal studies are costly, time-intensive, and raise several ethical concerns while cells cultured *in vitro* are not able to recapitulate tissue, organ, or organ system level responses to treatment [4]. A current major research thrust to improve the predictive power of early pharmacokinetic studies is the development of integrated organ-on-chip systems that ideally will better mimic organismal level responses to new treatments [3],[4].

While body-on-chip systems can potentially elucidate the pharmacokinetic parameters of a new drug throughout the body, they must first be tested against well-studied models, such as alcohol metabolism in the human body. The overall goal of such a project would be to connect organ-on-chip devices to create a whole-body response to a drug. However, we quickly realized that for the time we had to complete this project, and with the inability to carry out experiments in lab to validate some of our assumptions, our project would have to consist of examining just a few of the phenomena that would in theory form the bases for the organ-on-chip designs. Modeling the metabolism of alcohol throughout the body as a system of ODEs could be useful in recapitulating a system level response, however, what we're arguing is that valuable information could be learned from creating a system from the bottom-up that accurately captures behavior at the tissue level.

We focused on modeling three major separate steps in alcohol metabolism within the human body through the lens of an integrated organ-on-chip system. First, we looked at alcohol absorption and breakdown in the stomach, the mixing of alcohol from the 'bloodstream' into tissue, and the breakdown of alcohol in the liver. (Fig. 1).

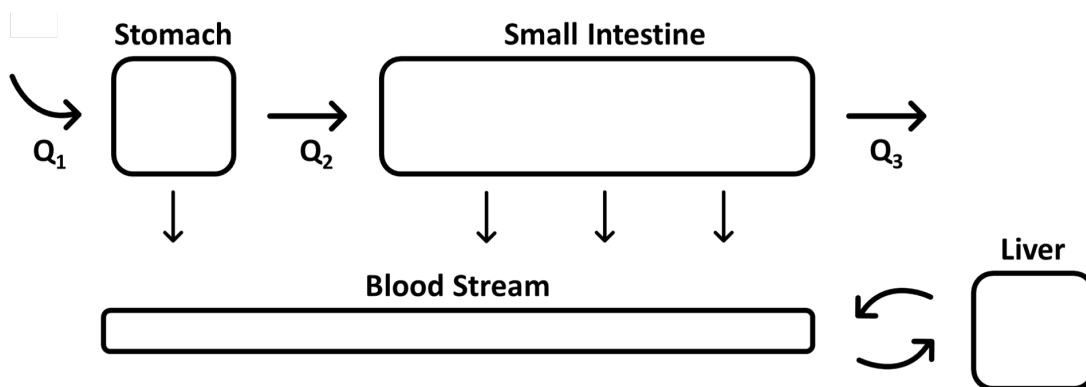


Fig. 1. Block diagram representation of alcohol's journey through a human body/body-on-chip system.

To ensure that the chip models alcohol metabolism in these three distinct regions correctly, a model for each region was created. These models are there to ensure fidelity of the chip. Once the models are complete a chip can be made that will use the data from the models to accurately

predict alcohol metabolism. Since alcohol metabolism is a well-studied pathway, models can be constructed, but more importantly the models can be compared against previous studies to ensure that they are accurate[B].

2 Methodology

2.1 Absorption Through the Small Intestine

Ethanol's first physiological step that we decided to try to model, is the small intestine. The stomach and the small intestine are interconnected so instead of doing one model for each, we modeled the small intestine, then we used the output of the stomach $k_s V_s$ as our left boundary value condition.[5]

To mathematically explain these series of steps

1. The ethanol concentration at the left boundary is the concentration being deposited by the stomach. Flux at the end of the intestine is zero, under the assumption that everything is absorbed before reaching the boundary.

$$\begin{aligned} E(0, t) &= k_s V_s \\ D \frac{dE}{dx}(L, t) &= 0 \end{aligned} \quad (1)$$

Where k_s is the rate(min^{-1}) at which the stomach empties into the small intestine, V_s is the volume of the stomach and D is the diffusivity constant

2. Initially nothing is consumed, therefore we have zero ethanol concentration.

$$E(x, t) = 0 \quad (2)$$

3. Ethanol absorption through the small intestine in one direction was modeled with the following equation"

$$\frac{dE}{dt} = -D \frac{d^2 E}{dx^2} \quad (3)$$

Solving the linear PDE we must obtain the total solution

$$E(x, t) = E_{\text{Homogeneous}} + E_{\text{particular}} \quad (4)$$

The homogeneous linear differential equation is described as

$$\frac{dE}{dt} = -D \frac{d^2 E}{dx^2} \quad (5)$$

and then a particular solution that satisfies Steady-state (Equation 6) was solved for.

$$\frac{dE}{dt} = 0. \quad (6)$$

It must be understood that since the boundary conditions are not homogeneous (zero boundary conditions) then there must be a particular solution.

Solving this simple linear PDE we take advantage of the technique known as, Separation of Variables.

To perform this technique first describe the temporal and spatial components of the PDE

$$\frac{d}{dt}\phi(x)G(t) = D\frac{d^2}{dx^2}\phi(x)G(t) \quad (7)$$

Next group the two by their respective space

$$\frac{1}{DG(t)} \frac{G(t)}{dt} = \frac{1}{\phi(x)} \frac{d^2\phi(x)}{d\phi(x)^2} = -\lambda \quad (8)$$

Understanding that the only way these two can equal one another is by both being constants, thus they must equal a constant $-\lambda$ We now begin solving the two separately

$$\frac{dG(t)}{dt} = -\lambda DG(t) \quad (9)$$

which equates to

$$G(t) = G(0)e^{-\lambda Dt} \quad (10)$$

giving us a function of time.

We proceed by evaluating the spacial double derivative

$$\frac{d^2\phi(x)}{d\phi(x)^2} = -\lambda\phi(x) \quad (11)$$

Assuming that $\lambda > 0$

$$\frac{d^2\phi(x)}{d\phi(x)^2} + \lambda\phi(x) = 0 \quad (12)$$

we can find a nontrivial solution to the problem

$$\phi(x) = A\cos(\sqrt{\lambda}x) + B\sin(\sqrt{\lambda}x) \quad (13)$$

where A and B are integration constants.

Utilizing the homogeneous boundary conditions a value can be found for the integration constants

$$E(0,t) = A\cos(0) + B\sin(0)$$

$$A = 0$$

$$E(X,t) = B\sin(\sqrt{\lambda}x)$$

$$\frac{dE}{dx}(L,t) = \sqrt{\lambda}B\cos(\sqrt{\lambda}L) \quad (14)$$

$$\sqrt{\lambda}L = \frac{(2n+1)\pi}{2}, n = 0, 1, 2, 3, etc.$$

$$\lambda = \left(\frac{(2n+1)\pi}{2L}\right)^2$$

Thus, describing the eigenmode expansion

$$E(x,t) = \sum_{n=0}^{\infty} B_n \sin\left(\frac{(2n+1)\pi}{2L}x\right) e^{-D\left(\frac{(2n+1)\pi}{2L}\right)^2 t} \quad (15)$$

Determining the particular solution is the next step in obtaining a total solution.

For this the boundary conditions that were previously discussed (1) will be taken into account and the assumption of steady state will be used as well

$$\begin{aligned} -D \frac{d^2 E}{dx^2} &= 0 \\ E(x) &= -\frac{C_1 x + C_2}{D} E(0) = -\frac{C_2}{D} \\ C_2 &= -k_s V_s D \\ \frac{dE}{dx}(L) &= -\frac{C_1}{D} \\ C_1 &= 0 \\ E_{particular} &= -k_s V_s D \end{aligned} \quad (16)$$

The total solution becomes (4)

$$E(x,t) = -DK_s V_s + \sum_{n=0}^{\infty} B_n \sin\left(\frac{(2n+1)\pi}{2L}x\right) e^{-D\left(\frac{(2n+1)\pi}{2L}\right)^2 t} \quad (17)$$

To solve for the remaining integration constant the initial conditions (2) will be utilized as well as the definition of orthogonality

$$\begin{aligned} E(x,0) &= DK_s V_s + \sum_{n=0}^{\infty} B_n \sin\left(\frac{(2n+1)\pi}{2L}x\right) \\ \left(\sum_{n=1}^{\infty} A_n \phi_n\right) \phi_m &= A_n \int_0^L \phi_n \phi'_m = \frac{L}{2} A_n \delta_{mn} \end{aligned} \quad (18)$$

By the definition of orthogonality

$$\begin{aligned} \int_0^L DK_s V_s \sin\left(\frac{(2n+1)\pi}{2L}x\right) &= B_n \int_0^L \sin\left(\frac{(2n+1)\pi}{2L}x\right) \sin\left(\frac{(2m+1)\pi}{2L}x\right) dx \\ B_n &= \frac{2DK_s V_s}{(2n+1)\pi} \left(\cos\left(\frac{(2n+1)\pi}{2}\right) - 1\right) \end{aligned} \quad (19)$$

Our total solution is

$$E(x,t) = -k_s V_s D + \sum_{n=0}^{\infty} \frac{2DK_s V_s}{(2n+1)\pi} \left(\cos\left(\frac{(2n+1)\pi}{2}\right) - 1\right) \sin\left(\frac{(2n+1)\pi}{2L}x\right) e^{-D\left(\frac{(2n+1)\pi}{2L}\right)^2 t} \quad (20)$$

Plotting the partial differential equation with Matlabs pdepe solver gave the following result. As shown by the graph there is a constant supply of mucosa into the small intestine. From there it gets quickly absorbed. According to the plot the ethanol doesnt travel very far down the intestine

before all of the ethanol gets removed from the small intestine (Fig. 2).

Limitations of Model

While trying to model ethanol digestion throughout the body several challenges were faced. For the PDE that modeled the small intestine, an analytical solution could not be achieved using Michaelis-Menton Kinetics for the source term. The source term that represented the emptying rate is dependent upon the concentration of ethanol in the stomach [6]. Some ethanol in the stomach is broken down by alcohol dehydrogenase 1C(ADH1C) [7]. After several attempts to solve using methods used in class and PDE solvers in MATLAB, the PDE was changed to make the equation easier to solve. The source term was eliminated, and the initial condition was changed to $k_s \cdot V_s$ for $x=0$ to reach an analytical solution. This new term K_s has a range of values but for the model it was assumed that the concentration of ethanol going into the stomach is a standard 0.3 mol per hour. A standard drink is one 12fl oz drink at 5 percent ethanol concentration. Doing stoichiometry a standard drink has 0.3 mol of ethanol. This allowed for the use of literature values for both k_s and V_s [5]. After the analytical solution was attained, modeling in MATLAB became troublesome. Initially the resulting graph showed an indefinite increase in concentration over time. However, the expected outcome should be an immediate decrease in concentration as the ethanol travels along the intestine. Therefore, by changing the source term and changing the initial conditions, a sensible graph was produced. This graph is still not completely accurate. From (Fig. 2) it can be seen that the initial concentration is constant through the time period. It should diminish over time since the initial input is one standard drink. It should only reset after an hour has passed, since that is when another drink would be consumed. Future modifications have to be made to include this periodicity and to include this diminishing over time.

2.2 Deposition of alcohol from blood into tissue

To understand the mass transport of alcohol from the blood into a tissue, we decided to base our model on a 2-D micromixer with parallel flows [8]. The micromixer would be used to add various concentrations of alcohol into our system at different times without increasing the total system volume and so we The channel has an overall width equal to W where the blood vessel is the region $0 < y < W/2$ and the tissue is the region $W/2 < y < W$ (assuming the diameter of the vessel is half our characteristic length). The blood enters the system with an initial concentration of alcohol c_0 while the tissue has an initially zero concentration of alcohol. The walls of the device are impermeable to alcohol. The fluid flow velocity within the system is equal to U and travels in the x -direction (Fig. 3).

We began with the equation for the conservation of mass in two dimensions

$$U \frac{\partial c}{\partial x} = D \left(\frac{\partial^2 c}{\partial x^2} + \frac{\partial^2 c}{\partial y^2} \right) \quad (21)$$

To make the system easier to analyze, we normalized our x and y values by dividing each by W and we normalized our concentrations by dividing by c_0 . When plugged into the above equation,

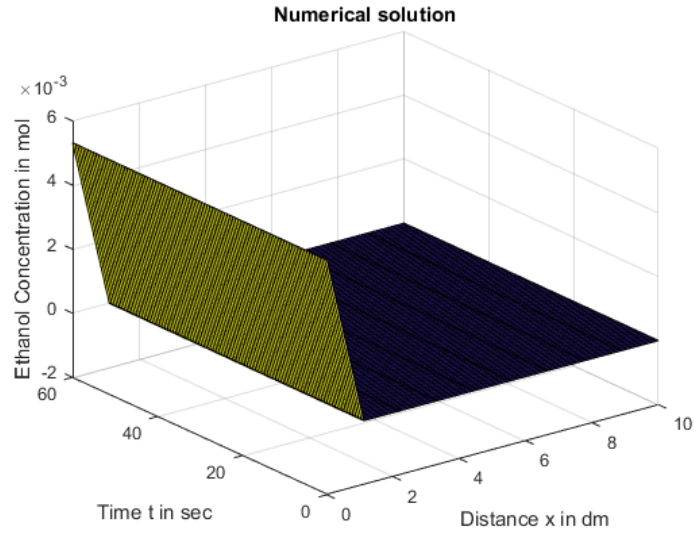


Fig. 2. Graphical representation of the small intestine

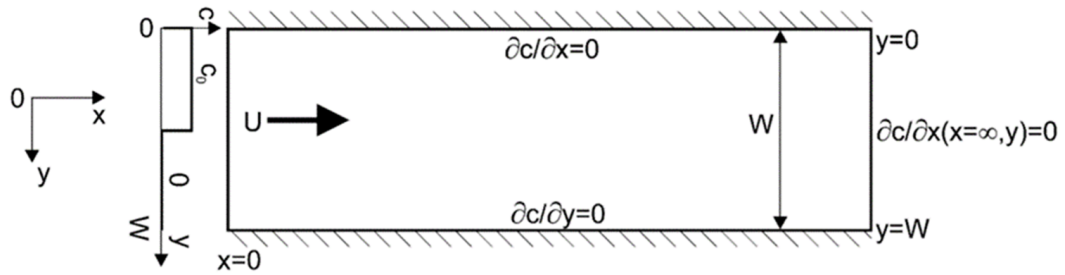


Fig. 3. Diagram of a 2-D microchannel mixer [5].

these normalized values (x^* , y^* , c^*) transform the equation into

$$Pe \frac{\partial c^*}{\partial x^*} = \frac{\partial^2 c^*}{\partial x^{*2}} + \frac{\partial^2 c^*}{\partial y^{*2}} \quad (22)$$

Where Pe is the Peclet number and is defined as $Pe = \frac{UW}{D}$ (Fig. 4).

To finish defining our system, we need our initial and boundary conditions. As described above, the initial conditions are

$$IC : \begin{cases} c^* \Big|_{x^*=0, 0 < y^* < 0.5} = 1 \\ c^* \Big|_{x^*=0, 0.5 < y^* < 1} = 0 \end{cases} \quad (23)$$

We are assuming no flux boundary conditions at the walls of the device but to fully describe the system we must also assume that as we progress along the vessels to infinity, the flux with respect to x becomes zero. *I.e.*

$$BC : \begin{cases} \frac{\partial c^*}{\partial y^*} \Big|_{y^*=0,1} = 0 \\ \frac{\partial c^*}{\partial x^*} \Big|_{x^* \rightarrow \infty} = 0 \end{cases} \quad (24)$$

As shown by Wu et al., separating the variables and applying the boundary and initial conditions provides us with the following equation

$$c^*(x^*, y^*) = \frac{2}{\pi} \sum_{n=1}^{\infty} \frac{\sin(n\alpha\pi)}{n} \cos(n\pi y^*) \exp\left(-\frac{2n^2\pi^2}{Pe + \sqrt{Pe^2 + 4n^2\pi^2}} x^*\right) + \alpha \quad (25)$$

In order to arrive at this solution, we assumed the diffusivity of alcohol must be the same in both the blood and tissue. To explore the limitations of this assumption, we plotted the solution if both channels were filled with blood and if both were tissue (Fig. 5).

The length a capillary travels in the x -direction should be many times the diameter of a capillary and so we evaluated the system at $x^* > 0$. For the system that is just alcohol in blood we see that by $x^* = 10$ the system has reached equilibrium and c^* across all y 's is uniform (Fig. 6).

Another thing we noticed is that the diffusion of alcohol in the tissue is much lower than in the blood. Because of this, as x^* increases the concentration of alcohol in the blood becomes uniform from $0 < y^* < 0.5$ while the concentration in the tissue is much more a gradient. To attempt to model this we stitched together the values of c^* from $0 < y^* < 0.5$ calculated with the diffusivity of alcohol in blood with the c^* from $0.5 < y^* < 1$. In order to ensure the total mass is balanced, the total concentration of alcohol at any location x^* was kept constant. The figure generated by doing this shows both that the c^* from $0 < y^* < 0.5$ equilibrates quickly while the c^* from $0.5 < y^* < 1$ is diffusion limited (Fig. 7).

We then verified that this assumption holds up as $x^* \rightarrow \infty$ (Fig. 8).

Limitations of Model

There are a few limitations of this model that would be interesting to explore further. First, the models are not symmetric around the point $y^* = 0.5$ (Fig. 9).

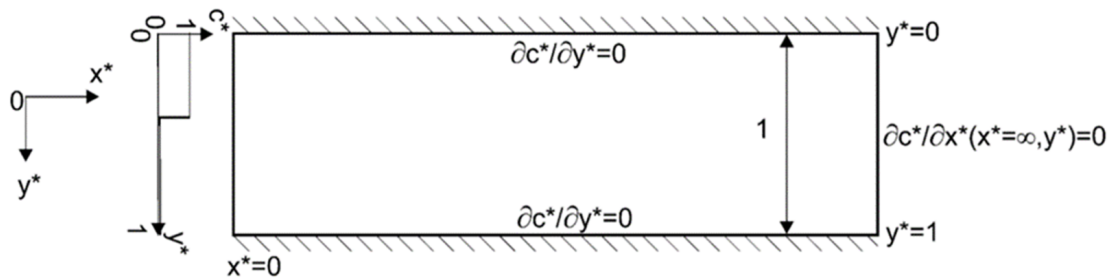


Fig. 4. Diagram of a 2-D microchannel mixer with normalized dimensions .

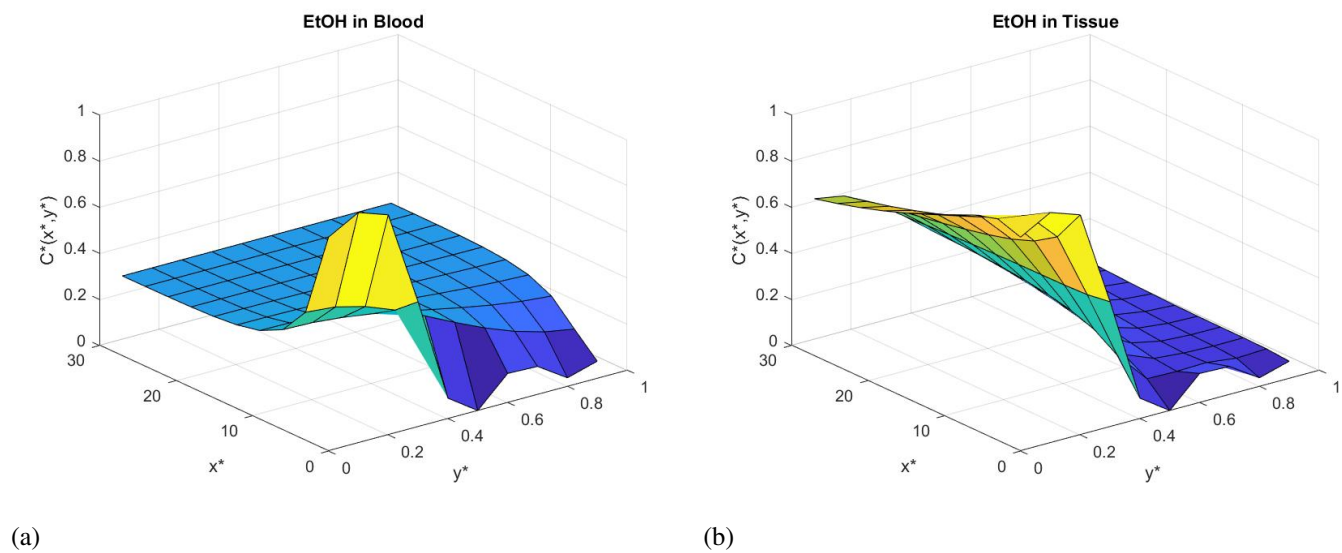


Fig. 5. Convection-Diffusion of alcohol in a 2-D microchannel mixer where both channels are filled with (a) blood and (b) tissue.

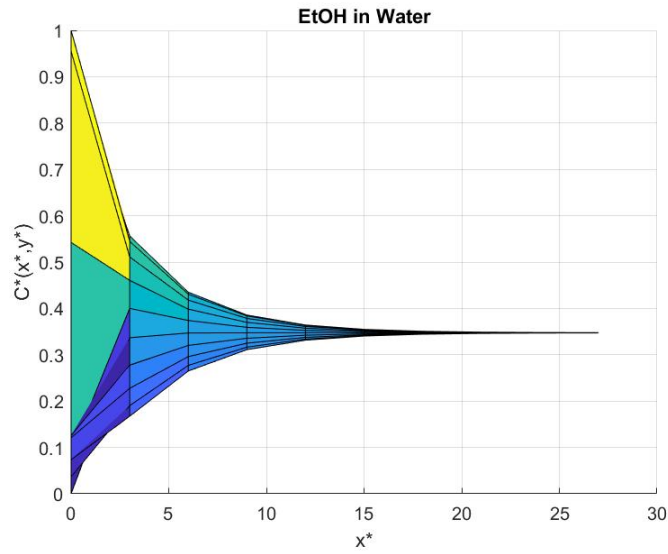


Fig. 6. Convection-Diffusion of alcohol in a 2-D microchannel mixer where both channels are filled with blood.

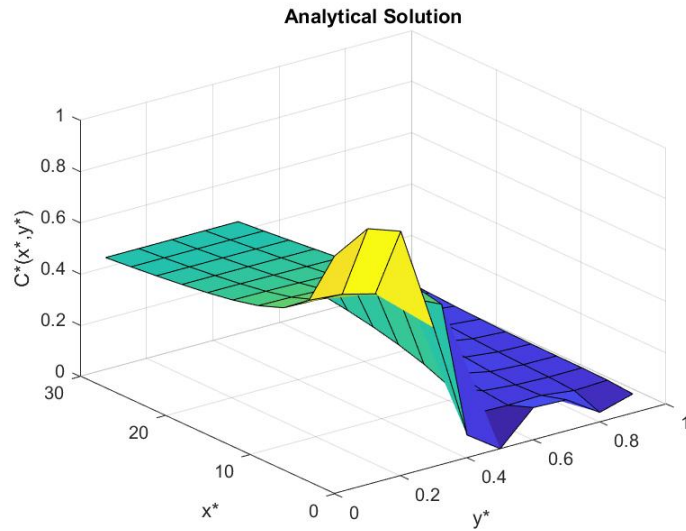
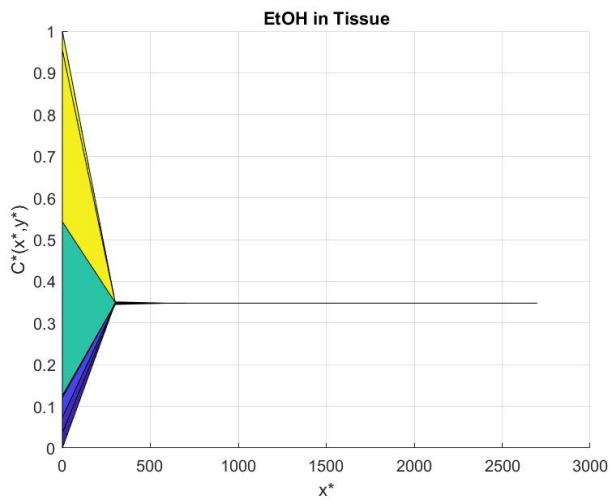
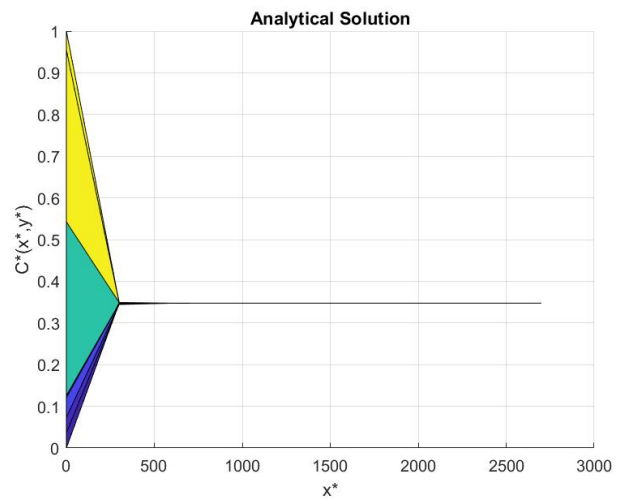


Fig. 7. Convection-Diffusion of alcohol in a 2-D microchannel mixer where one channel is filled with blood and the other is filled with tissue.

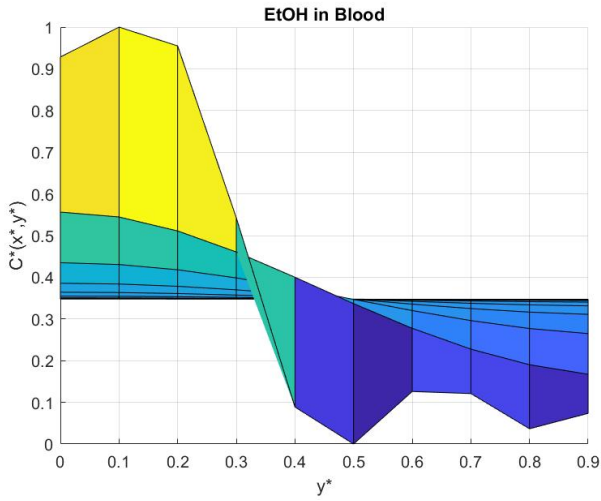


(a)

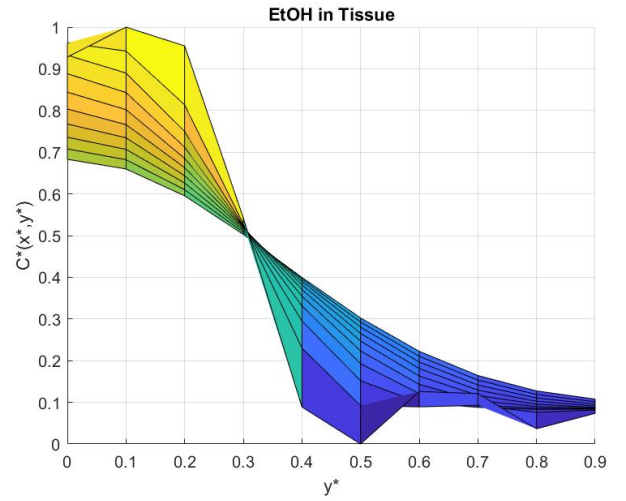


(b)

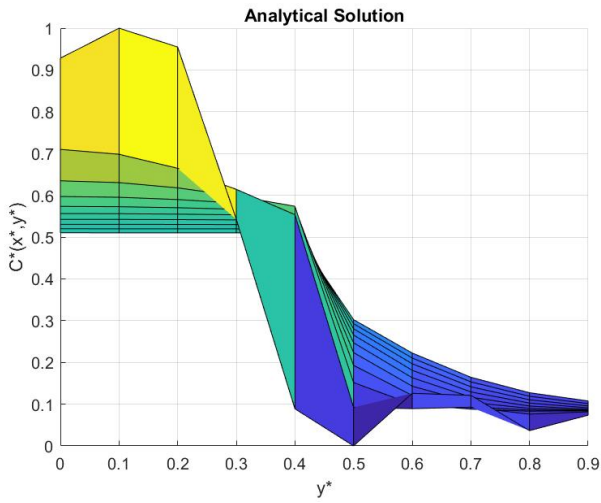
Fig. 8. Full-mixing assumption for large values of x^* .



(a)



(b)



(c)

Fig. 9. Asymmetry of the analytical solution around $y^* = 0.5$.

This then causes the equilibrium value of c^* at very large values of x^* to be lower than 0.5. We decided to accept this as a limitation of the model rather than to arbitrarily fix it by trimming our results and normalizing the graphs. Additionally, the way the c^* values from the two y^* regimes were stitched together doesn't take into account that there will be a lower driving force (lower c^* value) at $y^* = 0.5$. However, comparing the c^* values at different x^* points showed us that the value isn't ever more than 20% off so this won't affect our results too much, the system will just take longer to reach equilibrium.

2.3 Liver Absorption

Continuing on the physiological process, to mathematically describe the concentration of ethanol in the liver through time and space we make a few assumptions:

1. The concentration of ethanol at the walls of the liver are zero:

$$\begin{aligned} C_{Et}(0,t) &= 0 \\ C_{Et}(L,t) &= 0 \end{aligned} \quad (26)$$

2. There is a small concentration of ethanol in the liver initially:

$$C_{Et}(x,0) = C_{Et,0} \quad (27)$$

3. Ethanol is diffusing through the blood vessels into the liver via passive diffusion in one direction (Fick's Law):

$$\frac{dC_{Et}}{dt} = D \frac{d^2C_{Et}}{dx^2} \quad (28)$$

D refers to the diffusion coefficient, or the rate of diffusion.

4. Ethanol is consumed in the liver by Alcohol Dehydrogenase (ADH) via Michaelis Menten Kinetics

$$Q(x) = \frac{V_{max}C_{Et}(x)}{K_m + C_{Et}(x)} \quad (29)$$

k_m is the concentration which permits ADH to achieve half V_{max} . A low k_m indicates that ADH is generally saturated with Ethanol, thus, a reaction will occur more or less at a constant rate.

V_{max} refers to the maximum rate of reaction when ADH has been saturated with Ethanol, this can be evaluated by:

$$V_{max} = k_{cat}C_{Et,0} \quad (30)$$

k_{cat} describes the turnover rate of the ADH-Ethanol complex to Acetaldehyde.

With the given assumptions we come to our governing equation that describes the concentration of ethanol in the liver through time and space

$$\frac{dC_{Et}}{dt} = D \frac{d^2C_{Et}}{dx^2} - \frac{V_{max}C_{Et}(x)}{K_m + C_{Et}(x)} \quad (31)$$

To solve this linear PDE we must obtain a total solution

$$C_{Et}(x,t) = C_{Et,Homogeneous} + C_{Et,Particular} \quad (32)$$

The homogeneous linear differential equation is described as the following

$$\frac{dC_{Et}}{dt} = D \frac{d^2 C_{Et}}{dx^2} \quad (33)$$

For the particular solution the assumption of steady state is made, at an infinite amount of time the amount of ethanol diffusing into the liver will no longer depends on time

$$D \frac{d^2 C_{Et}}{dx^2} = \frac{V_{max} C_{Et}(x)}{k_m + C_{Et}(x)} \quad (34)$$

However, when attempting to solve for the particular solution it can be concluded that there is no analytical solution to describe the total solution of this model

$$\frac{C_{Et}(x,t)(2k_m \log(C_{Et}(x,t) + C_{Et}(x,t) - 2k_m))}{2V_{max}} = \frac{x^2}{2D} + C_1 x + C_2 \quad (35)$$

Although, a total solution can not be found, the homogeneous solution (45) can be expressed analytically through the technique previously described, Separation of Variables

$$\frac{d}{dt} \phi(x)G(t) = D \frac{d^2}{dx^2} \phi(x)G(t) \quad (36)$$

$$\frac{1}{DG(t)} \frac{G(t)}{dt} = \frac{1}{\phi(x)} \frac{d^2 \phi(x)}{d\phi(x)^2} = -\lambda \quad (37)$$

$$\frac{dG(t)}{dt} = -\lambda DG(t) \quad (38)$$

$$G(t) = G(0)e^{-\lambda Dt} \quad (39)$$

$$\frac{d^2 \phi(x)}{d\phi(x)^2} = -\lambda \phi(x) \quad (40)$$

$$\frac{d^2 \phi(x)}{d\phi(x)^2} + \lambda \phi(x) = 0 \quad (41)$$

$$\phi(x) = A \cos(\sqrt{\lambda}x) + B \sin(\sqrt{\lambda}x) \quad (42)$$

Using the assumption we made about out the boundaries (26) we begin to solve for A and B

$$\begin{aligned} \phi(0) &= 0 \\ \phi(0) &= A \cos(0) + B \sin(0) \\ A &= 0 \end{aligned} \quad (43)$$

$$\begin{aligned}
\phi(L) &= 0 \\
\phi(L) &= B\sin(\sqrt{\lambda}L) \\
\sqrt{\lambda}L &= n\pi, n = 1, 2, 3, \text{etc.} \\
\lambda &= \left(\frac{n\pi}{L}\right)^2
\end{aligned} \tag{44}$$

Thus, our general eigenmode expansion to the homogeneous equation is

$$Ct_{Et,Homo}(x,t) = \sum_{n=1}^{\infty} B_n \sin\left(\frac{n\pi}{L}x\right) e^{-D\left(\frac{n\pi}{L}\right)^2 t} \tag{45}$$

In the following steps orthogonality will be assumed to solve for the remaining integrating constant

$$\left(\sum_{n=1}^{\infty} A_n \phi_n\right) \phi_m = A_n \int_0^L \phi_n \phi'_m = \frac{L}{2} A_n \delta_{mn} \tag{46}$$

To solve for our integration constant the initial conditions (27) will be considered

$$Ct_{Et}(x,0) = \sum_{n=2}^{\infty} B_n \sin\left(\frac{n\pi}{L}x\right) = Ct_{Et,0} \tag{47}$$

By taking advantage of orthogonality (46) finding a solution for B_n is now possible

$$\begin{aligned}
\sum_{n=2}^{\infty} B_n \sin\left(\frac{n\pi}{L}x\right) \sin\left(\frac{m\pi}{L}x\right) &= Ct_{Et,0} \sin\left(\frac{m\pi}{L}x\right) \\
\int_0^L B_n \sin\left(\frac{n\pi}{L}x\right) \sin\left(\frac{m\pi}{L}x\right) dx &= \int_0^L Ct_{Et,0} \sin\left(\frac{m\pi}{L}x\right) dx \\
B_n &= \frac{2}{L} Ct_{Et,0} \int_0^L \sin\left(\frac{m\pi}{L}x\right) dx \\
B_n &= -\frac{2Ct_{Et,0}}{\pi n} (\cos(n\pi) - 1), n = 1, 2, 3, \text{etc.}
\end{aligned} \tag{48}$$

Thus, the homogeneous solution for the eigenmode expansion becomes

$$Ct_{Et,Homo}(x,t) = \sum_{n=1}^{\infty} \frac{2Ct_{Et,0}}{\pi n} (\cos(n\pi) - 1) \sin\left(\frac{n\pi}{L}x\right) e^{-D\left(\frac{n\pi}{L}\right)^2 t}, n = 1, 2, 3, \text{etc.} \tag{49}$$

Limitations of Model

The model has several issues. The first and most evident is the inability to analytically solve for the consumption of ethanol by ADH inside the liver. The inability to model the consumption creates a number of flaws, if consumption is not taken into account the model suggest that the ethanol will merely sit in the liver with no repercussions. As it is well known the liver is responsible for metabolizing the ethanol for elimination.

Another issue with the model is the inability to model diffusion in multiple direction. By just assuming that the ethanol is diffusing in just one direction you limit the model to fully define the system [9],[10],[11],[12],[13].

3 Conclusion

Ultimately, our major concerns with our project arise from the simplifying assumptions made to analytically solve our models. Because organ-on-chip technology is so new, it was difficult to find literature confirming that the assumptions made to adapt the pharmacological response of an organ, such as the liver, into a chip-based system are valid. What further complicates the matter is that while there is a lot of literature on alcohol metabolism, these papers only address problems alcohol can cause. That is to say, virtually all of these papers focus on blood alcohol concentration and how quickly a person becomes sober while we were more interested in what the alcohol concentration in tissues and organs does over time and how they travel from one compartment to the other. Future directions that we would be interested in exploring would be aimed at better mimicking physiological conditions on chips. That is to say, in retrospect, having a well-defined system greatly simplifies the work that needs to be done to create analytical models.

Bibliography

- [1] E. W. Esch, A. Bahinski and D. Huh, "Organs-on-chips at the frontiers of drug discovery," *Nature Reviews Drug Discovery*, vol. 14, no. 4, pp. 248-260, 20 3 2015.
- [2] H. E. Abaci and M. L. Shuler, "Human-on-a-chip design strategies and principles for physiologically based pharmacokinetics/pharmacodynamics modeling.," *Integrative biology : quantitative biosciences from nano to macro*, vol. 7, no. 4, pp. 383-91, 4 2015.
- [3] "Could organs-on-chips replace drug testing on animals?," [Online]. Available: <https://www.elsevier.com/connect/could-organs-on-chips-replace-drug-testing-on-animals>.
- [4] H. Ledford, "Translational research: 4 ways to fix the clinical trial," *Nature*, vol. 477, no. 7366, pp. 526-528, 28 9 2011.
- [5] M. D. Levitt, R. Li, E. G. DeMaster, M. Elson, J. Furne and D. G. Levitt, "Use of measurements of ethanol absorption from stomach and intestine to assess human ethanol metabolism.," *The American journal of physiology*, vol. 273, no. 4 Pt 1, pp. G951-7, 10 1997.
- [6] S. Zakhari, "Overview: how is alcohol metabolized by the body?," *Alcohol research & health : the journal of the National Institute on Alcohol Abuse and Alcoholism*, vol. 29, no. 4, pp. 245-54, 2006.
- [7] D. M. Umulis, N. M. Gürmen, P. Singh and H. S. Fogler, "A physiologically based model for ethanol and acetaldehyde metabolism in human beings," *Alcohol*, vol. 35, no. 1, pp. 3-12, 1 2005.
- [8] Z. Wu and N.-T. Nguyen, "Convective–diffusive transport in parallel lamination micromixers," *Microfluidics and Nanofluidics*, vol. 1, no. 3, pp. 208-217, 10 7 2005.
- [9] A. I. Cederbaum, "Alcohol Metabolism," *Clinics in Liver Disease*, vol. 16, no. 4, pp. 667-685, 11 2012.
- [10] W. C. Kerr and T. K. Greenfield, "The average ethanol content of beer in the U.S. and individual states: estimates for use in aggregate consumption statistics.," *Journal of studies on alcohol*, vol. 64, no. 1, pp. 70-4, 1 2003.
- [11] M. D. Schmidt, R. R. Vallabhajosyula, J. W. Jenkins, D. Calvetti, A. Kuceyeski and E. Somersalo, "A mathematical model of liver metabolism: from steady state to dynamic Automated refinement and inference of analytical models for metabolic networks A mathematical model of liver metabolism: from steady state to dynamic," *Journal of Physics Conference Series J. Phys.: Conf. Ser.*, vol. 124.
- [12] C. M. Oneta, U. A. Simanowski, M. Martinez, A. Allali-Hassani, X. Parés, N. Homann, C. Conradt, R. Waldherr, W. Fiehn, C. Coutelle and H. K. Seitz, "First pass metabolism of ethanol is strikingly influenced by the speed of gastric emptying.," *Gut*, vol. 43, no. 5, pp. 612-9, 11 1998.